

## Global Phase Diagram for the Wetting Transition at Interfaces in Fluid Mixtures

María Eugenia Costas, Carmen Varea, and Alberto Robledo

*División de Estudios de Posgrado, Facultad de Química, Universidad Nacional Autónoma de México, México 04510, D.F., Mexico*

(Received 24 January 1983; revised manuscript received 4 October 1983)

The authors analyze the wetting behavior at interfaces of three-phase equilibria exhibited by a fluid with two independent densities when described in mean field. The calculation treats nonuniformities exactly and regions are identified in interaction space where first- or second-order transitions or no transitions occur. Sullivan's model of the fluid-solid interface is obtained as a limiting case, but the global phase diagram is qualitatively different from that pertaining to a system described by one bulk order parameter plus two surface fields.

PACS numbers: 68.10.Cr

Our understanding of the phenomena of wetting in terms of the structure and thermodynamics of the interfaces involved stems from the phenomenological work of Widom and Cahn.<sup>1</sup> Both new insight and new questions, still to be answered by experiment, have arisen since.<sup>2-7</sup> The most significant effort to obtain a statistical-mechanical description of the wetting transition has been the study of model systems with one bulk order parameter in contact with an inert phase or wall that introduces one<sup>2</sup> or two<sup>3-5</sup> additional surface parameters. The global behavior of this class of systems, i.e., the possibility of first- or second-order perfect-to-partial wetting transitions, prewetting transitions, and associated surface critical phenomena, is now well understood.<sup>4,5</sup> Here we briefly communicate the wetting properties of another model whose global behavior does not coincide with that of the above systems. This model corresponds to the thermodynamic formulas of the van der Waals (vdW) binary mixture,<sup>8,9</sup> and is described by a two-component order parameter in the absence of external (surface) fields under the restriction that the range of the interaction potentials is the same for like and unlike pairs. The wetting transition associated with models of fluid-fluid interfaces has already been calculated in the square-gradient approximation<sup>6</sup> and also studied with a very similar density functional scheme as described here.<sup>7</sup> Here we attempt to construct a

“global interfacial phase diagram” by studying the interfacial properties as a function of the interaction potential parameters. In contrast to the one-density fluid model against a wall, the restriction on the ranges of the attractive interactions to be the same does not suppress the appearance of different types of behavior. It has been shown<sup>3,5</sup> that the relative ranges of the solid-fluid and fluid-fluid potentials play a crucial role in determining the order of the wetting transition. Tarazona, Telo da Gama, and Evans<sup>7</sup> have also considered the dependence of the order of the transition on the relative range of like and unlike pairs for certain model fluid mixtures. We studied the model for the range of values of the parameters  $\Lambda$  and  $\zeta$  of van Konynenburg and Scott<sup>10</sup> for which the equal-diameter mixture exhibits three-phase equilibria terminating at only one (upper) critical end point (UCEP).  $\Lambda$  and  $\zeta$  provide, respectively, a measure of heat of mixing and critical-point separation of the pure components, and therefore with a similar characterization of real binary mixtures contact can be established with experimental results.<sup>11</sup>

The calculation, which is exact<sup>8</sup> in the limit of one-dimensional infinitely ranged interactions and not restricted to the square-gradient approximation, begins with the consideration of Kac-type pair potentials between like and unlike pairs and leads to the following (nonlocal) expressions for the density functional:

$$\beta\Omega = \int dr \left\{ f(\rho_i(r)) + \frac{1}{4} \sum_{i,j=1,2} \alpha_{ij} \int dr' \exp(-|r-r'|) [\rho_i(r) - \rho_i(r')] [\rho_j(r) - \rho_j(r')] - \sum_i \mu_i \rho_i(r) \right\}, \quad (1)$$

where

$$\beta f(\rho_i) = \rho \ln(1 - \sigma\rho) + \sum_{i=1,2} \rho_i (1 - \ln \rho_i) + \beta \sum_{i,j=1,2} \alpha_{ij} \rho_i \rho_j, \quad \rho = \rho_1 + \rho_2,$$

and where the  $\alpha_{ij}$  are the interaction parameters,  $\sigma$  the molecular diameter of both types of molecules,  $\mu_i$  the chemical potentials, and  $\beta$  the inverse temperature. In terms of the  $\alpha_{ij}$  we have that  $\Lambda = (\alpha_{11})$

$+ \alpha_{22} - 2\alpha_{12})/(\alpha_{11} + \alpha_{22})$  and  $\zeta = (\alpha_{22} - \alpha_{11})/(\alpha_{11} + \alpha_{22})$ . The associated equations for the profiles are solved under the conditions that phase equilibria is possible among three phases. The interfacial tensions are subsequently determined as the excess free energy.

In general, and within the accuracy of our numerical calculations, two sets of density profiles are obtained for each of the three possible interfaces of a three-phase state (in the absence of gravity). One of them is always the composite of the profiles for the two other interfaces that satisfies the boundary conditions of the interface of interest. This solution describes, therefore, a wetting film. The other solution participates in the description of partial wetting. In what follows we describe the wetting types found with the help of interfacial tension versus temperature plots. Figure 1(a) represents a symmetrical mixture with an ordinary UCEP,  $0 < \Lambda < 0.3478$  and  $\zeta = 0$ . The tensions  $\sigma_{\alpha\gamma}$  and  $\sigma_{\beta\gamma}$  are identical for all  $T$  and greater than  $\sigma_{\alpha\beta}$  (the liquid-liquid interface); the wetting film structure has always the largest tension. Figure 1(b) corresponds to mixtures with the geometric-mean combining rule,  $\zeta^2 + (\Lambda - 1)^2 = 1$ , and, as shown by Sullivan,<sup>9</sup> the  $\alpha\gamma$  interface has only one possible structure, this being the composite of the  $\alpha\beta$  and  $\beta\gamma$  profiles. The system exhibits perfect-wetting states for all  $T \leq T_c$ . Figure 1(c) describes mixtures for which phase equilibria occur with total segregation or immiscibility of the components. This requires that, say,  $\alpha_{22} \rightarrow \infty$ , so that  $\Lambda = 1$  and  $\zeta = 1$ . The other two parameters, or, what matters, their ratio  $\alpha_{12}/\alpha_{11}$  remains underdetermined. This is

the system that maps into Sullivan's model for the solid-fluid interface<sup>2</sup> with  $\alpha_{12}$  identified as the fluid-to-wall interaction  $\epsilon$ . The density profile  $\rho_2(r)$  is always a step function, while that for  $\rho_1(r)$  is the fluid-to-wall profile described in Ref. 2. At low temperatures there exist two different structures for the  $\alpha\gamma$  interface, the film always with the largest tension. The two tensions join tangentially at a transition temperature  $T_w \leq T_c$ , the value of which is determined by  $\alpha_{12}/\alpha_{11}$ . For temperatures  $T > T_w$  only the film structure persists. The system exhibits a second-order wetting transition. Figure 1(d) represents the behavior for mixtures in the region in  $(\Lambda, \zeta)$  space bounded by the symmetrical and the geometric-mean mixtures, i.e.,  $\zeta^2 + (\Lambda - 1)^2 < 1$  and  $\Lambda < 1$ . For these mixtures there exist two distinct structures for the  $\alpha\gamma$  interface for every  $T < T_c$ . At low temperatures the largest tension corresponds to the film structure and at temperatures closer to  $T_c$  the situation is reversed and the film becomes the equilibrium state. The transition at  $T_w$  is first order. There is a corresponding latent heat and the two interface structures can coexist at  $T_w$  in regions separated by contours with a positive line tension. Figure 1(e) corresponds to mixtures bounded by the geometric-mean mixtures and the limiting case  $\alpha_{11} = 0$ , i.e.,  $\zeta^2 + (\Lambda - 1)^2 > 1$ ,  $\zeta \leq 1$ , and  $\Lambda > 0$ . There exist two distinct solutions for the  $\alpha\gamma$  interface for all  $T \leq T_c$  but the wetting film tension is always the smaller. Finally, the dotted curve in the  $\Lambda$ - $\zeta$  plot of Fig. 1 divides  $(\Lambda, \zeta)$  space into two regions. Above this line the interface that experiences the transition is of the liquid-liquid type and below the line it is of the liquid-vapor type. The curve originates, within the precision of our calculations, at the center of the so-called shield region,<sup>10</sup> where the three-phase line splits into three branches at high temperatures, and terminates at  $\Lambda = \zeta = 1$ , where the perfect-wetting and nonwetting regimes reported in Ref. 2 correspond to the two possibilities mentioned. The mixtures on the dotted curve have the behavior shown in Fig. 1(a).<sup>12</sup>

Tarazona *et al.*<sup>7</sup> have found a second-order transition in a model mixture with equal-ranged potentials that falls in our region *d* ( $\Lambda = 0.204$  and  $\zeta = 0.095$ ); however, we note an important difference between the respective model mixtures. Our calculations correspond to the exact density functional of the one-dimensional Kac potential mixture in the vdW limit, where the range of the repulsions is reduced to a point on the scale in

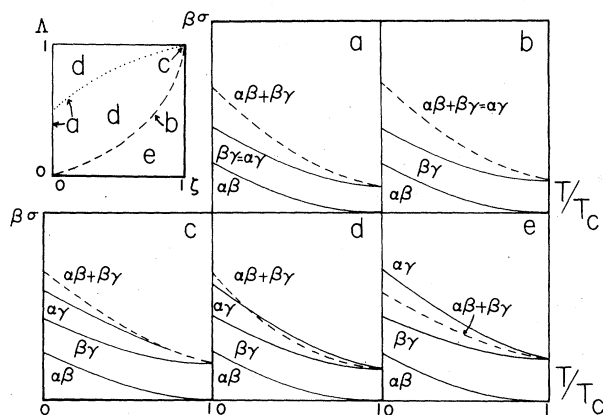


FIG. 1. The interaction space  $(\Lambda, \zeta)$  of the van der Waals binary mixture and the temperature behavior of interfacial tensions at three-phase states for the different interaction regions shown.

which the attractions and the density profiles vary. This has the effect<sup>8</sup> that, while the contribution to the functional arising from the repulsions becomes local in position, the integrations in the term representing the attractions range from zero to infinite separation of the two particles, and not from the hard-core diameter (closest contact in the original scale before taking the vdW limit). The difference in the integral equations for the profiles is not negligible and this must account for our finding a first-order transition for these same values of  $\Lambda$  and  $\zeta$ .

The tensions  $\sigma_{\beta\gamma}$ ,  $\sigma_{\alpha\gamma}$ , and  $\sigma_{\alpha\beta+\beta\gamma}$  in Fig. 1 are all drawn to meet tangentially at  $T_c$ . Since  $\sigma_{\alpha\beta}$  vanishes with (classical, in this case) exponent  $\mu = \frac{3}{2}$  at  $T_c$ , the film tension  $\sigma_{\alpha\beta+\beta\gamma}$  joins  $\sigma_{\beta\gamma}$  with the same exponent. To find how  $\sigma_{\alpha\gamma}$  approaches  $\sigma_{\beta\gamma}$  (when it is different from  $\sigma_{\alpha\beta+\beta\gamma}$  near  $T_c$ ) we look at the density expansion of their difference. The lowest-order terms in  $|T - T_c|$  for  $\Delta\sigma = \sigma_{\alpha\gamma} - \sigma_{\beta\gamma}$  can be found by expansion of Eq. (1) under the condition of stationarity. We obtain

$$\Delta\sigma \sim \int dr \sum_{i,j,k} \frac{\partial^3 f_h}{\partial \rho_i \partial \rho_j \partial \rho_k} \delta\rho_i \delta\rho_j \delta\rho_k + \dots, \quad (2)$$

where  $f_h$  is the contribution to  $f$  from the hard-core repulsions and  $\delta\rho_i$  is the difference in density  $i$  between the  $\alpha\gamma$  and  $\beta\gamma$  profiles. When the critical end point is approached only one of the two correlation lengths associated with the profiles diverges, and a linear transformation re-

lates  $\rho_1$  and  $\rho_2$  with the normal density variables  $\eta_1$  and  $\eta_2$ , each of which responds to only one of the correlation lengths. Rewriting Eq. (2) in terms of these variables we obtain for the temperature dependence of  $\Delta\sigma$  around  $T_c$  the form  $\Delta\sigma \sim |T - T_c|^{3/2}$ . This result is consistent with the recently derived<sup>13</sup> general proof on the tangency of  $\Delta\sigma$  for systems under the square-gradient approximation.

The locus of the transition temperature in  $(\Lambda, \zeta)$  space, shown in Fig. 2, is composed of three surfaces; two of them appear at opposite sides of the  $\zeta = 0$  axis and correspond to wetting at liquid-vapor interfaces, and the third represents wetting at the liquid-liquid interface. The surfaces meet at  $T = T_c$  along ridges where the two liquid-vapor interfaces or a liquid-vapor and the liquid-liquid interfaces have the same tensions for all  $T \leq T_c$  (they represent mixtures with partial wetting for all  $T \leq T_c$ ). There, the perfect- and partial-wetting tensions become tangent at  $T = T_c$  and hence we identify these ridges as loci of critical wetting transitions that we denote as Sp (special points). The three surfaces meet in the shield region where the three Sp lines merge. This point is therefore a wetting multicritical point that we label SR for shield region. Two other multicritical points appear associated with the Sp lines, located at the common terminus of these and the lines of continuous wetting transitions at  $\Lambda = \pm \zeta = 1$ ; we label them PI for perfect immiscibility. In Fig. 3 we show different sec-

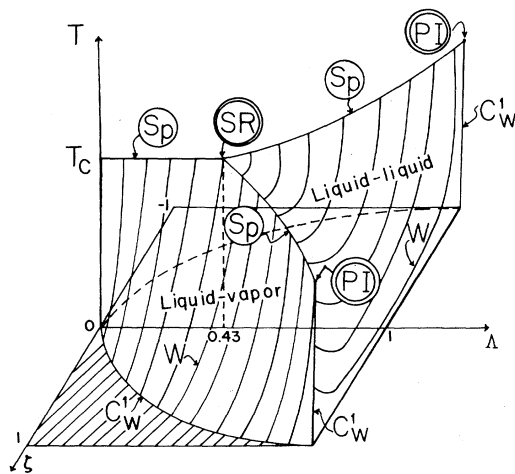


FIG. 2. The interfacial transition temperature at three-phase coexistence in interaction space  $(\Lambda, \zeta)$  showing wetting surfaces  $W$ , critical lines  $C_w^1$ , and multicritical points (encircled labels).

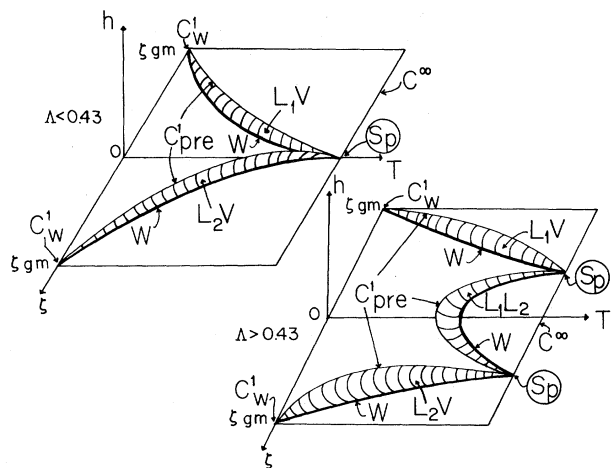


FIG. 3. Sections of the global interfacial phase diagram showing wetting lines  $W$ , critical lines  $C_{pre}^1$ ,  $C_w^1$ , and  $C^\infty$ , and multicritical points (encircled labels).  $h$  represents the departure from three-phase states along two-phase coexistence loci.

tions at constant  $\Lambda$  of Fig. 2 where in addition we represent prewetting<sup>4</sup> transitions and their associated interfacial critical points. The variable  $h$  represents the departure in  $(\mu_1, \mu_2)$  space along two-phase lines from the three-phase point at  $T$ . Prewetting occurs at only one of the three two-phase lines for a given mixture and in the figure, where we have followed the nomenclature of Ref. 4, we indicate the type of two-phase line to which  $h$  refers in the different regions. We observe that the Sp points (as in Ref. 4) constitute the common terminus of the wetting and critical prewetting lines, and hence the SR point is in turn a higher-order multicritical point, the common end of the three different Sp lines.

The model mixture is limited by construction to the regime of marginal surface enhancements,<sup>4</sup>  $g_{ij} = 0$ , since the particle interaction cannot experience relaxation at interfacial regions relative to their bulk values. Also, only in the limiting case  $\Lambda = \pm \zeta = 1$  can the ratios  $\alpha_{ij}/\alpha_{ii}$  be related to a surface incremental field. For these reasons the model does not exhibit the characteristic behavior induced by surface enhancements and fields. On the contrary, the restriction ensures that the wetting properties found, such as the SR and PI multicritical points, are due only to the consideration of a two-component order parameter.

We wish to thank John Kerins for informative and stimulating discussions. We acknowledge financial support by Consejo Nacional de Ciencia y Tecnología de México.

<sup>1</sup>B. Widom, J. Chem. Phys. **62**, 1332 (1975), and Phys. Rev. Lett. **34**, 999 (1975), and J. Chem. Phys. **68**, 3878 (1978); J. W. Cahn, J. Chem. Phys. **66**, 3667 (1977). See also C. Ebner and W. F. Saam, Phys. Rev. Lett. **38**, 1486 (1977), who discovered a surface wetting transition with the employment of density functional theory.

<sup>2</sup>D. E. Sullivan, Phys. Rev. B **20**, 3991 (1979), and J. Chem. Phys. **74**, 2604 (1981).

<sup>3</sup>G. F. Teletzke, L. E. Scriven, and H. T. Davis, J. Chem. Phys. **77**, 5794 (1982), and **78**, 1431 (1983).

<sup>4</sup>H. Nakanishi and M. E. Fisher, Phys. Rev. Lett. **49**, 1565 (1982).

<sup>5</sup>R. Pandit and M. Wortis, Phys. Rev. B **25**, 3226 (1982); R. Pandit, U. Schick, and M. Wortis, Phys. Rev. B **26**, 5112 (1982); E. H. Hauge and M. Shick, Phys. Rev. B **27**, 4288 (1983).

<sup>6</sup>M. M. Telo da Gama and R. Evans, Mol. Phys. **48**, 251 (1983).

<sup>7</sup>P. Tarazona, M. M. Telo da Gama, and R. Evans, Mol. Phys. **49**, 283 (1983).

<sup>8</sup>C. Varea, A. Valderrama, and A. Robledo, J. Chem. Phys. **73**, 6265 (1980).

<sup>9</sup>D. E. Sullivan, J. Chem. Phys. **77**, 2632 (1982).

<sup>10</sup>R. L. Scott and P. H. van Konynenburg, Discuss. Faraday Soc. **49**, 81 (1970); P. H. van Konynenburg and R. L. Scott, Philos. Trans. Soc. London, Ser. A **298**, 495 (1980).

<sup>11</sup>J. W. Schmidt and M. R. Moldover, J. Chem. Phys. **79**, 379 (1983).

<sup>12</sup>The symmetrical mixtures with  $0.4664 < \zeta < 1$  show the behavior labeled *d*. Because of the multiplicity of three-phase lines the mixtures in the shield region, including the symmetrical ones with  $0.3478 < \zeta < 0.4664$ , show a more complex behavior not reported here.

<sup>13</sup>M. Robert and P. Tavan, J. Chem. Phys. **78**, 2557 (1983).